PNAS
www.pnas.org

Supplementary Information for

Distinct Metabolic Adaptation of Liver Circadian Pathways to Acute and Chronic Patterns of Alcohol Intake

Jonathan Gaucher, Kenichiro Kinouchi, Nicholas Ceglia, Emilie Montellier, Shahaf Peleg, Carolina Magdalen Greco, Andreas Schmidt, Ignasi Forne, Pierre Baldi, Selma Masri, Axel Imhof and Paolo Sassone-Corsi

Paolo Sassone-Corsi
Email: psc@uci.edu

This PDF file includes:

Supplementary text
Figures S1 to S5
Legends for Datasets S1 to S7

Other supplementary materials for this manuscript include the following:

Datasets S1 to S7

www.pnas.org/cgi/doi/10.1073/pnas.1911189116

Supplementary Information Text

Metabolic Cage Analysis

Indirect calorimetry was performed by negative-flow system cages Oxymax/CLAMS (Columbus Instruments). Feeding and lighting conditions in metabolic cages were the same as those in the normal housing cages. Feeder counts less than 0 g or more than 1.0 g per 10 min during *ad libitum* fed experiment were excluded from the study.

Locomotor Activity Analysis

Mice were individually housed under 12hour light/ 12hour dark schedule. Locomotor activity was measured using optical beam motion detection (Philips Respironics). Data was collected using the Minimitter VitalView 5.0 data acquisition software. Actograms and activity profiles were computed using Clocklab software (Actimetrics).

Plasma ALT measurement

Plasma Alanine Transaminase (ALT) activity was measured by fluorometric assay according to the manufacturer's protocols (Abcam, ab105134).

Cytokine Profiling

A total of 31 mouse cytokines were profiled using a multiplex immunoassay platform, and data were extracted based on cytokine-specific standards by Eve Technologies (Calgary, Canada). Six independent plasma samples were used from mice with chronic control and EtOH treatments. Cytokines with more than three replicates out of range were eliminated from the analysis. Any data more than 1.5 interquartile ranges above the third quartile or below the first quartile were defined as outliers and excluded from the analysis.

Protein extraction

For total liver protein extracts, the protocol was adapted from (1) with the following modifications. 50mg of liver was homogenized in Denaturation Buffer (500mM Tris-HCl pH 6.8, 500 mM NaCl, 20% Glycerol, 1% NP40, 0.1% SDS, 1% beta-mercaptoethanol, 0.22 µM TSA, 10 mM Nicotinamide, 20 mM NaF, 0.5 mM PMSF and Complete protease inhibitor (Roche, 04693132001)) or modified RIPA Buffer (10 mM Tris-HCl pH8, 150 mM NaCl, 1% NP40, 0.5% DOC, 5 mM $MgCl_2$, 0.22 µM TSA, 10 mM Nicotinamide, 20 mM NaF, 0.5 mM PMSF and Complete protease inhibitor (Roche, 04693132001)).

For fractionated protein extracts, the protocol was adapted from (2), (3). Briefly, 150 mg of liver was homogenized in TMS Buffer (50 mM Tris-HCl pH8, 5 mM $MgCl_2$, 250 mM 20% Sucrose, 0.22 µM TSA, 10 mM Nicotinamide, 20 mM NaF, 0.5 mM PMSF and Complete protease inhibitor (Roche, 04693132001)), pass through a 100 µm filter and centrifuged at 800 g at 4°C. The pellet contains the nuclei and the supernatant is enriched with the cytoplasm. The cytoplasmic supernatant was centrifuged at 11000g at 4°C, the resulting supernatant constitutes the cytosolic fraction and the pellet containing the mitochondria was further washed with TMS Buffer,

centrifuged at 11000g at 4°C and resuspended in Denaturation Buffer to constitute the mitochondrial fraction. The nuclear pellet was washed in HKSN Buffer (10 mM HEPES-NaOH, 25 mM KCl, 0.65 mM Spermidine, 1 mM EDTA, 1 mM EGTA, 0.34 M Sucrose, 1% NP40, 1 mM DTT, 0.22 μM TSA, 10 mM Nicotinamide, 20 mM NaF, 0.5 mM PMSF and Complete protease inhibitor (Roche, 04693132001)), centrifuged at 800 g at 4°C, resuspended in Denaturation Buffer, and sonicated to constitute the nuclear fraction.

Western blots analysis

Generally, 20 μg of total liver protein extract or 5 μg of fractionated protein extracts was loaded on 6%–12% polyacrylamide gels. Antibodies used for western blots are as follows: anti-BMAL1 (Abcam, ab93806), anti-COX IV (Abcam, ab14744), anti-REV-ERBα (Cell Signaling Technology, 13418), anti-acetylated lysine (Cell Signaling, 9441), anti-CRY1 (Bethyl Laboratories, A302-614), anti-PER2 (Alpha Diagnostic, PER21-A), anti-acetylated BMAL1 (Millipore, AB15396), anti-ACTIN (Abcam, ab3280), anti-α-TUBULIN (Sigma, T5168) and anti-p84 (Genetex, 5E10). The blots were scanned and densitometry was analyzed through ImageJ software.

RNA sequencing analysis

- mRNA sequencing

Total RNA was monitored for quality control using the Agilent Bioanalyzer Nano RNA chip and Nanodrop absorbance ratios for 260/280 nm and 260/230 nm. Library construction was performed according to the Illumina TruSeq mRNA stranded protocol. The input quantity for total RNA was 0.75 μg and mRNA was enriched using oligo dT magnetic beads. The enriched mRNA was chemically fragmented for four minutes. First strand synthesis used random primers and reverse transcriptase to make cDNA. After second strand synthesis the ds cDNA was cleaned using AMPure XP beads and the cDNA was end repaired and then the 3’ ends were adenylated. Illumina barcoded adapters were ligated on the ends and the adapter ligated fragments were enriched by nine cycles of PCR. The resulting libraries were validated by qPCR and sized by Agilent Bioanalyzer DNA high sensitivity chip. The concentrations for the libraries were normalized and then multiplexed together. The concentration used for clustering the flowcell was 200 pM. The multiplexed libraries were sequenced on eight lanes using single end 100 cycles chemistry for the HiSeq 4000. The version of HiSeq control software was HCS 3.3.76 with real time analysis software, RTA 2.7.6.

- Alignment and Expression Normalization

Sequencing data for 72 samples in FastQ format was produced using post-processing from Illumina software CASAVA 1.8.2 by the Genomics High-Throughput Facility at the University of California, Irvine. Reads failing Illumina's standard quality tests were not included in these FastQ files. The sequencing reads from each sample in the experiment were separately aligned to the reference genome mm10 and corresponding known splice junctions extracted from the UCSC Genome Browser (http://genome.ucsc.edu/) (4), (5) using the short-read aligner ELAND v2e (Illumina). Reads aligned with a non-unique best match or with two or more mismatches with the reference sequences were discarded from the analyses. The remaining uniquely aligned reads were used to estimate relative transcript abundance for further analysis. Reads per Kilobase of transcript per Million mapped reads (RPKM) were used to quantify the relative abundance of each transcript in a sample and to perform gene expression analyses.

Acetylome and Proteome Analysis

- Sample preparation and mass spectrometry for acetylome analysis

The acetylome protocol was adapted from (6, 7) with the following modifications. 500 mg of liver tissue were homogenized in 1.4 ml homogenizing buffer (50 mM Tris–HCl pH 7.5, 500 mM NaCl, 1 mM EDTA, 0.1% NP-40, and 20% glycerol) in the presence of 15 mM sodium butyrate and 60 µM of sirtinol (Tocris) and then added with 200 µl of freshly de-ionized 6 M urea/2 M thiourea. Following sonication, 5 µl of benzonase was added for 1 hour. The proteins were digested for 4 h with 10 µg of Lys-C (Wako) at 25°C, with the addition of a final concentration of 40 mM ammonium bicarbonate. Following the incubation, urea was diluted x8 to a final concentration of 1M by the addition of ammonium bicarbonate to a final concentration of 40 mM followed by overnight incubation (ON) with 300 µg trypsin (Worthington). The isolated peptides were desalted and the peptide amount was measured by a NanoDrop (Thermo Fischer Scientific). Equal amounts of peptides were enriched for acetylated peptides using Acetyl Lysine Antibody beads (Immunechem, ICP0388) overnight. Beads were washed 4 times in PBS–Tween 0.1% followed by 4 washes in PBS. Finally, peptides were eluted with 125 µl of TFA 0.1%. Following desalting, the eluted peptides were dissolved in 10 µl of 0.1% formic acid for LC-MS/MS analysis.

As input, an aliquot of each sample was taken before the enrichment for acetylated lysines and was diluted in TFA 0.1% and around 40 µg was desalted and concentrated. From the resulting samples, 1.5 µg was analyzed by mass spectrometry as described below.

- Acetylome mass spectrometry

To identify and quantify protein acetylations, 5 µl of the desalted sample were directly loaded onto the analytical C18 column (150x0.075 mm, Reprosil C18-AQ, 2.4 µM, Dr. Maisch GmbH) packed into an ESI emitter tip employing a flow rate of 300 nl/min of 96% LC solvent A (0.1% FA in H2O) and 4% solvent B (80% ACN, 20% H2O, 0.1% FA) for 5 min. Peptides were separated by a linear gradient from 4% B to 50% B in 90 min, followed by 7 min high organic wash and column reconstitution. Throughout the entire run eluting peptides were directly ionized and analyzed on QExactive HF mass spectrometer (Thermo-Fisher Scientific). The mass spectrometer was operated in a TOP10 duty cycle in positive ionization mode acquiring peptide precursor ions from 375 to 1600 m/z in the survey scan and performing up to 10 MS/MS scans on selected precursor ions. MS/MS precursors required a charge state of 2+ to 5+, were subsequently isolated in a 1.7 Da window and fragmented at a normalized collision energy (NCE) of 28%. MS/MS spectra were acquired at a resolution of 15000 at 200 m/z. Precursors were excluded from repeated fragmentation for 20s, to avoid redundancy.

- Identification of acetylated peptides

Mass spectrometry data were searched against a mouse protein database (Uniprot 05/2015) using the Andromeda algorithm within the Maxquant software suite (vs. 1.5.3.12) employing a forward/reversed search strategy (8, 9). Settings for peptide identification were cleavage by trypsin/P with up to 3 missed cleavages, carbamidomethylation of Cys as fixed modification and Oxidation (M); Acetyl (Protein N-term);Acetyl (K);Phospho (STY) as variable modification in the main search. All obtained peptide hits were filtered for a false discovery rate of 2% with a minimal identification score of 10 for unmodified peptides and 35 for modified sequences. Proteins hits were filtered to 5% FDR. To facilitate quantitation, the “match between runs” option was enabled within an alignment time window of 10 min before and 1.5 min after retention time alignment. Peptide intensities were reported as arbitrary units (counts/time), protein intensities were normalized to the protein size as iBAQ values.

Statistical Analysis

The time series of abundance estimates for each transcript were then used to identify and describe oscillating transcripts using BioCycle (10) with results corroborated using JTK-Cycle (11). Oscillating transcripts in the final analysis were determined using a P-value cutoff of 0.01 and we report only the results obtained with BioCycle. Heat maps were generated by R package 'gplots'. Gene Set Enrichment Analysis was performed to determine whether or not a specific subset of genes are enriched either in control or ethanol fed mice (12). Gene sets with false discovery rate of less than 25% were considered significantly enriched. Differential analysis of protein expression levels between conditions was performed with a Bayesian-regularized t-test using CyberT (13), (14). Analysis on differential acetylation of proteins were implemented according to the previously described method (7). Adjusted P-values of less than 0.05 were considered significant and used for the heatmaps. Graphs were depicted using Microsoft Excel, GraphPad Prism 7, and Adobe Illustrator CS6.

- Functional Analysis

The Database for Annotation, Visualization and Integrated Discovery (DAVID) (15), (16) pathway analysis tool was used to identify GO terms related to biological process and potentially enriched pathways in sets of oscillating transcripts, differentially acetylated proteins, and differentially expressed proteins.

- Transcriptional Regulation

Transcription factor and RNA-binding protein (RBP) binding site enrichment was performed using a combination MotifMap (17), (18) and publicly available ChIP-Seq datasets from ENCODE (5), and MotifMap-RNA (19). Enriched binding sites were identified upstream of oscillating transcript sets through MotifMap and MotifMap-RNA with a FDR < 0.25 and BBLS > 1.0. Enriched binding sites from ChIP-Seq experiments were found using a standard Fisher test with a P-value cutoff of 0.01. All enrichment scores were calculated using the mm10 reference genome as a background. Transcription regulation of targeted transcripts for individual transcription factors (TF) and RBPs was identified using a combination of the tools listed above and the predicted phase produced for oscillating transcripts from BioCycle. Oscillating transcription factors and RBPs found to be in-phase or anti-phase with a known target were identified as being directly regulated in a circadian fashion.

- Visualization

Analysis was performed using pipelines implemented for the Circadiomics (20), (21) database and web portal (circadiomics.ics.uci.edu) where all the transcriptomic data associated with this work is publicly available.

Fig. S1

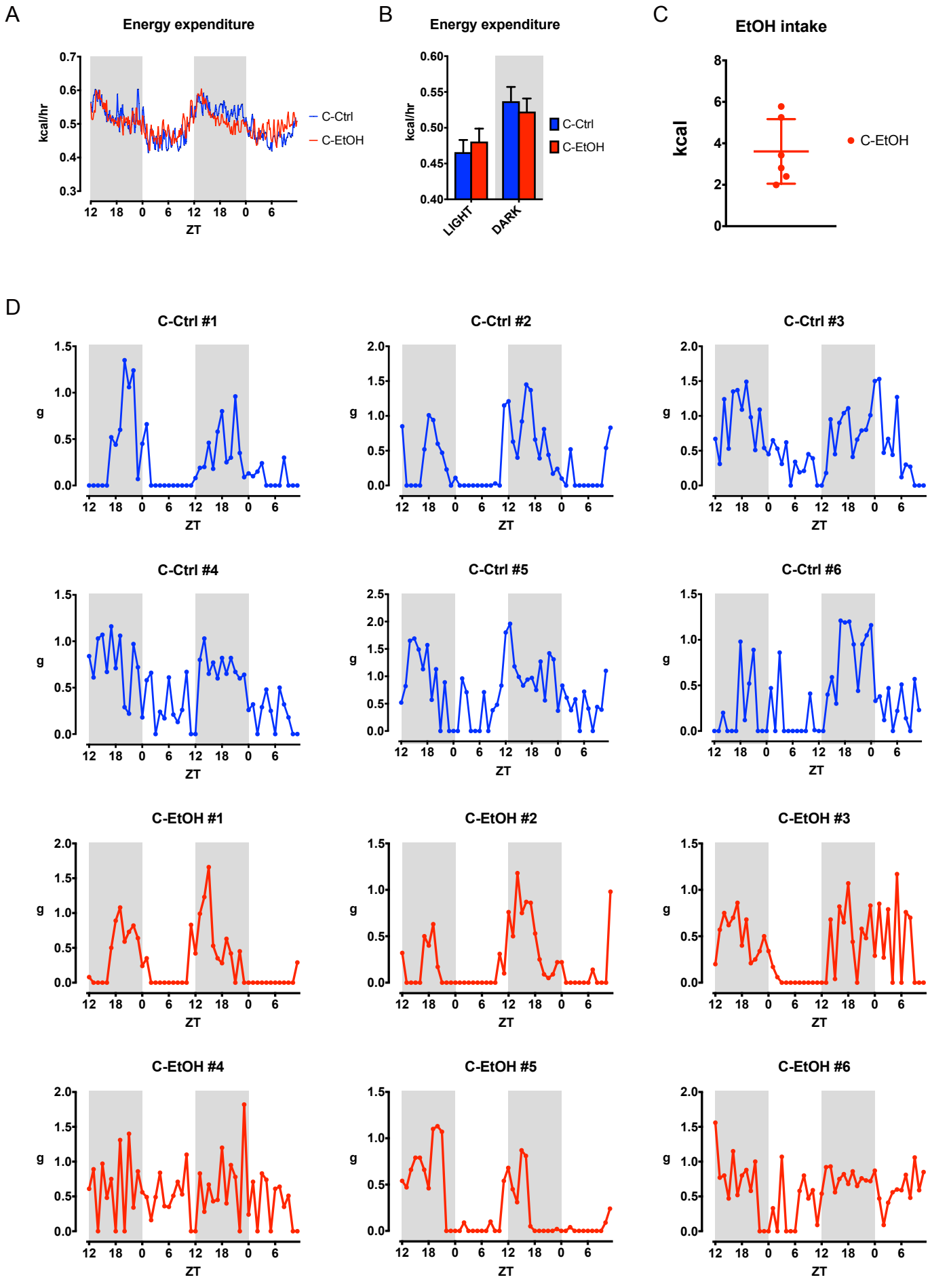
A
Energy expenditure
kcal/hr
ZT
C-Ctrl
C-EtOH
B
Energy expenditure
kcal/hr
LIGHT
DARK
C-Ctrl
C-EtOH
C
EtOH intake
kcal
C-EtOH
D
C-Ctrl #1
C-Ctrl #2
C-Ctrl #3
C-Ctrl #4
C-Ctrl #5
C-Ctrl #6
C-EtOH #1
C-EtOH #2
C-EtOH #3
C-EtOH #4
C-EtOH #5
C-EtOH #6
g
ZT

Fig. S1. Alcohol-induced circadian disruption of metabolism and behavior, related to Fig. 1.

(A, B) Metabolic cage analysis (n=6 per group) showing the time-series of energy expenditure over a 48 hr period (left panel) and the average of energy expenditure over the light and dark periods (right panel). (C) The cumulative ethanol intake over a 24 hr period estimated from intake of the liquid diet. (D) Food intake for individual mice over a 48 hr period.

Fig. S2

A

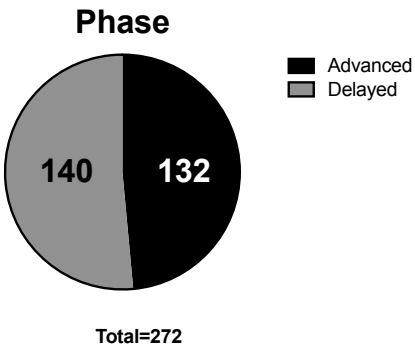

B

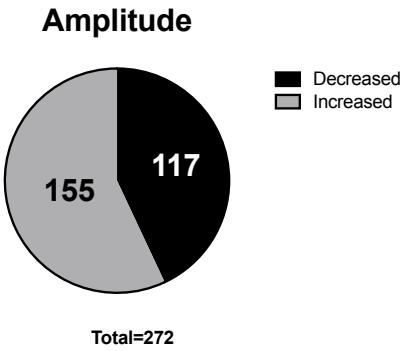

C

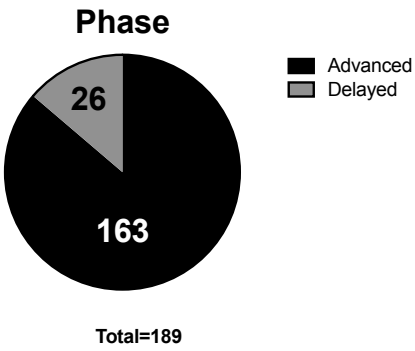

D

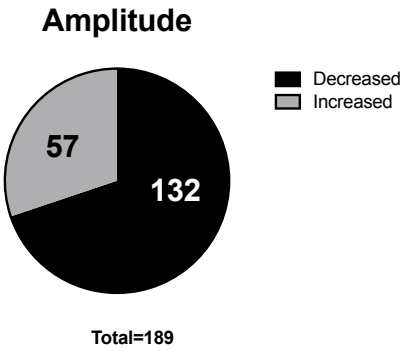

E

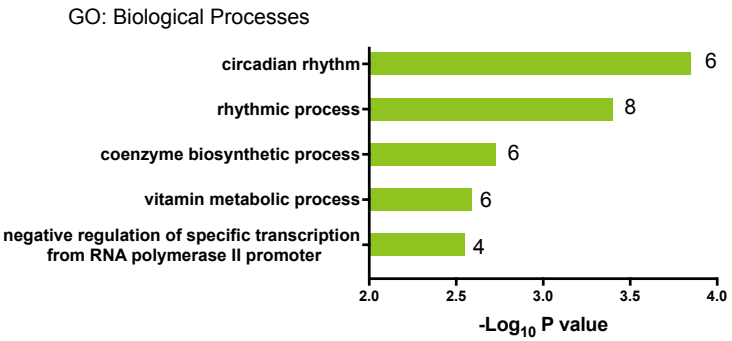

F

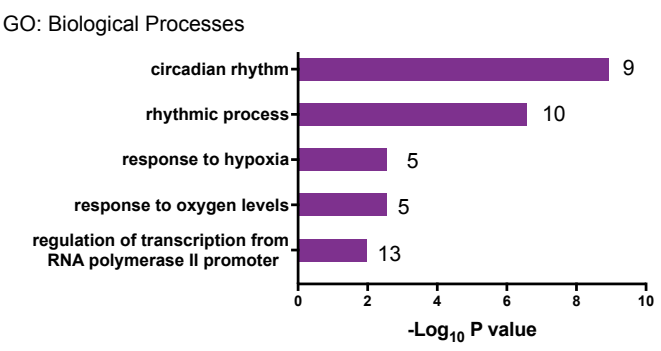

Fig. S2. Distinct reprogramming of hepatic circadian transcriptome by acute and chronic ethanol feeding, related to Fig. 2.

(A) Pie chart showing the phase of the rhythmic genes in acute ethanol (EtOH) mice compared to acute control (Ctrl) mice. (B) Pie chart showing the amplitude of the rhythmic genes in acute EtOH mice compared to acute Ctrl mice. (C) Pie chart showing the phase of the rhythmic genes in chronic EtOH mice compared to chronic Ctrl mice. (D) Pie chart showing the amplitude of the rhythmic genes in chronic EtOH mice compared to chronic Ctrl mice. (E) Gene ontology analysis showing the top five biological processes enriched in the rhythmic genes oscillating both in acute Ctrl and EtOH groups, with the number of genes indicated on the graph. (F) Gene ontology analysis showing the top five biological processes enriched in the rhythmic genes oscillating both in chronic Ctrl and EtOH groups, with the number of genes indicated on the graph.

Fig. S3

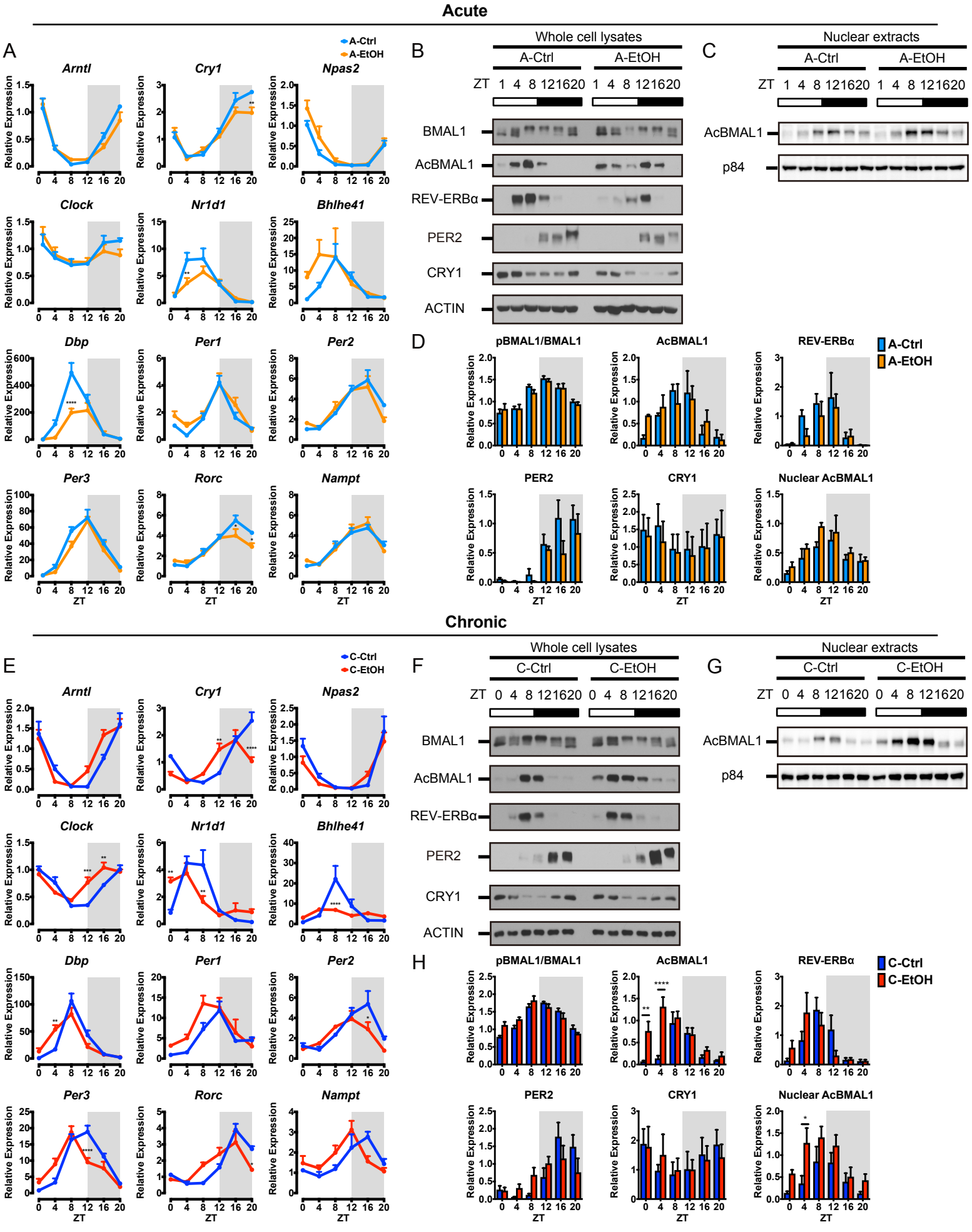
Acute
A
A-Ctrl
A-EtOH
Arntl
Cry1
Npas2
Clock
Nr1d1
Bhlhe41
Dbp
Per1
Per2
Per3
Rorc
Nampt
Relative Expression
ZT
B
Whole cell lysates
A-Ctrl
A-EtOH
ZT 1 4 8 121620 1 4 8 121620
BMAL1
AcBMAL1
REV-ERBα
PER2
CRY1
ACTIN
C
Nuclear extracts
A-Ctrl
A-EtOH
ZT 1 4 8 121620 1 4 8 121620
AcBMAL1
p84
D
pBMAL1/BMAL1
AcBMAL1
REV-ERBα
A-Ctrl
A-EtOH
PER2
CRY1
Nuclear AcBMAL1
Chronic
E
C-Ctrl
C-EtOH
Arntl
Cry1
Npas2
Clock
Nr1d1
Bhlhe41
Dbp
Per1
Per2
Per3
Rorc
Nampt
Relative Expression
ZT
F
Whole cell lysates
C-Ctrl
C-EtOH
ZT 0 4 8 121620 0 4 8 121620
BMAL1
AcBMAL1
REV-ERBα
PER2
CRY1
ACTIN
G
Nuclear extracts
C-Ctrl
C-EtOH
ZT 0 4 8 121620 0 4 8 121620
AcBMAL1
p84
H
pBMAL1/BMAL1
AcBMAL1
REV-ERBα
C-Ctrl
C-EtOH
PER2
CRY1
Nuclear AcBMAL1

Fig. S3. Alcohol-induced circadian disruption of core clock genes, related to Fig. 3.

(A) Gene expression profiles of core clock genes in acute ethanol (EtOH) feeding. (B) Representative immunoblots of liver whole cell lysates with acute EtOH feeding. (C) Representative immunoblots of liver nuclear extracts with acute EtOH feeding. (D) Quantitation of the blot band density in Figs. S3B and C, presented as mean + SEM. (E) Gene expression profiles of core clock genes in chronic EtOH feeding. (F) Representative immunoblots of liver whole cell lysates with chronic EtOH feeding. (G) Representative immunoblots of liver nuclear extracts with chronic EtOH feeding. (H) Quantitation of the blot band density in Figs. S3F and G, presented as mean + SEM. Gene expression was normalized to 18S ribosomal RNA and presented as mean + SEM (n=4-6 biological replicates per time point per group). Protein expression was normalized to ACTIN or p84 and presented as mean + SEM (n=3 biological replicates per time point per group). *P<0.05, **P<0.01, ***P<0.001, ****P<0.0001 in ANOVA with Bonferroni post-hoc test.

Fig. S4

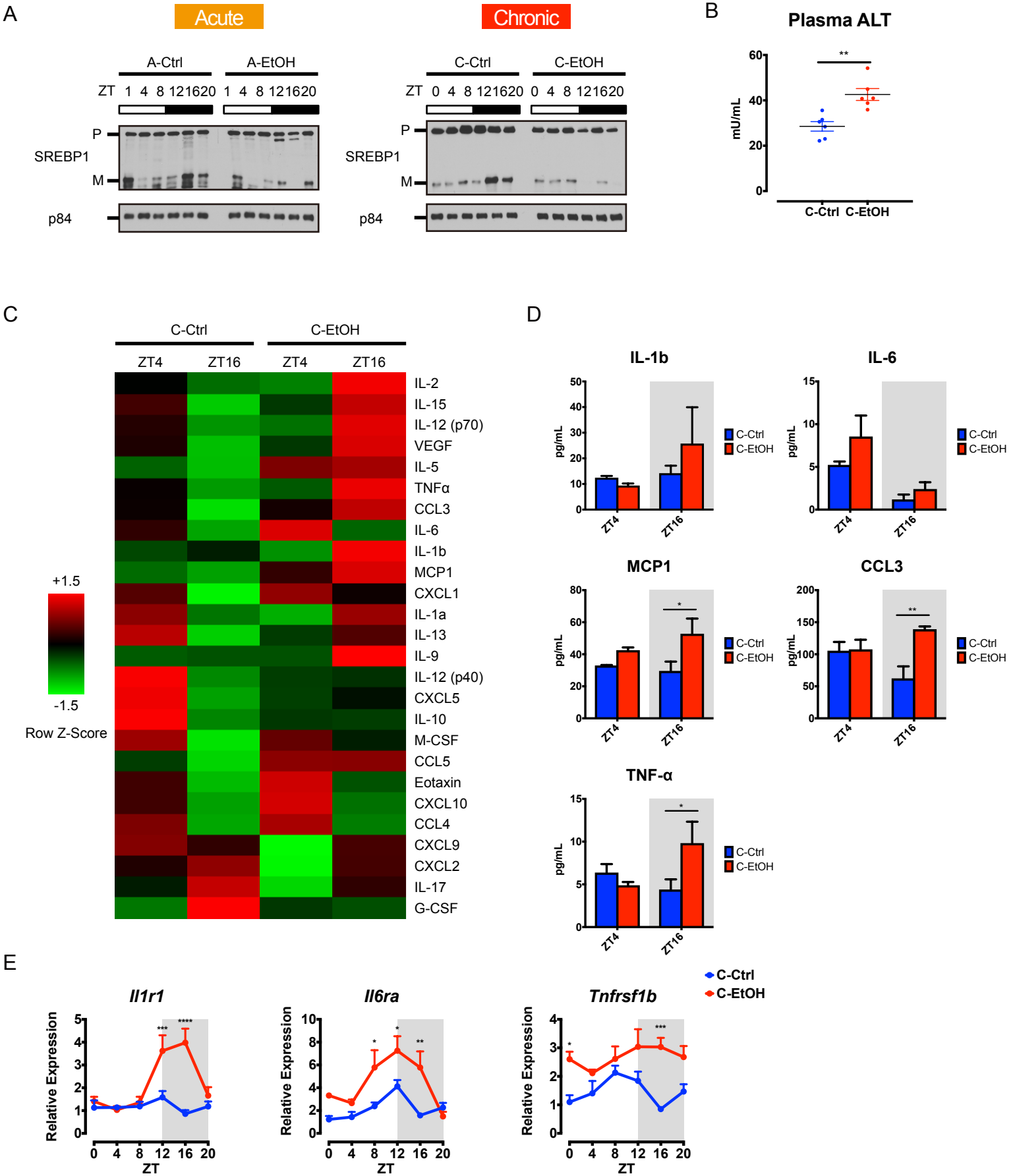
A
Acute
Chronic
A-Ctrl
A-EtOH
ZT 1 4 8 121620 1 4 8 121620
P
SREBP1
M
p84
C-Ctrl
C-EtOH
ZT 0 4 8 121620 0 4 8 121620
B
Plasma ALT
mU/mL
C-Ctrl C-EtOH
C
C-Ctrl
C-EtOH
ZT4 ZT16 ZT4 ZT16
IL-2
IL-15
IL-12 (p70)
VEGF
IL-5
TNFα
CCL3
IL-6
IL-1b
MCP1
CXCL1
IL-1a
IL-13
IL-9
IL-12 (p40)
CXCL5
IL-10
M-CSF
CCL5
Eotaxin
CXCL10
CCL4
CXCL9
CXCL2
IL-17
G-CSF
+1.5
-1.5
Row Z-Score
D
IL-1b
IL-6
MCP1
CCL3
TNF-α
pg/mL
C-Ctrl
C-EtOH
ZT4
ZT16
E
Il1r1
Il6ra
Tnfrsf1b
Relative Expression
ZT
C-Ctrl
C-EtOH

Fig. S4. Ethanol differentially alters SREBP-mediated circadian pathway, related to Fig. 4.

(A) Representative immunoblots of hepatic nuclear SREBP1 expression with acute (left panel) and chronic (right panel) EtOH feeding. (B) Plasma alanine aminotransferase (ALT) levels from mice under chronic control and chronic EtOH conditions. Data are shown as mean ± SEM (n=6 biological replicates per group). **P<0.01 in unpaired t test. (C) Plasma cytokine analysis was performed using plasma from chronic control and chronic EtOH feeding collected at ZT4 and ZT16, and displayed as a heat map. (D) Profiles of inflammatory cytokines from plasma with chronic control and EtOH feeding collected at ZT4 and ZT16. Data are shown as mean + SEM (n=3~6 biological replicates per time point per group). (E) Gene expression profiles of cytokine receptor genes in chronic EtOH feeding. Gene expression was normalized to 18S ribosomal RNA and presented as mean + SEM (n=4-6 biological replicates per time point per group). *P<0.05, **P<0.01, ***P<0.001, ****P<0.0001 in ANOVA with Bonferroni post-hoc test.

Fig. S5

A

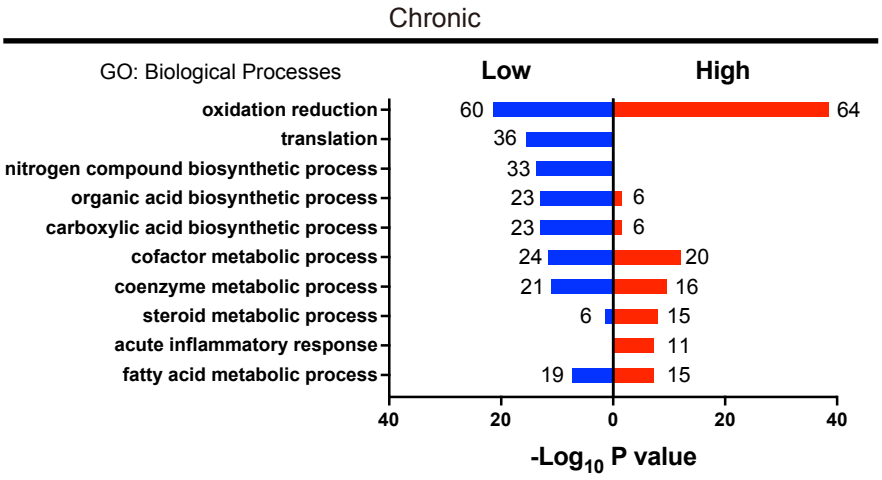
Chronic
GO: Biological Processes
Low
High
oxidation reduction
translation
nitrogen compound biosynthetic process
organic acid biosynthetic process
carboxylic acid biosynthetic process
cofactor metabolic process
coenzyme metabolic process
steroid metabolic process
acute inflammatory response
fatty acid metabolic process
60
64
36
33
23
6
23
6
24
20
21
16
6
15
11
19
15
40
20
0
20
40
-Log10 P value

B

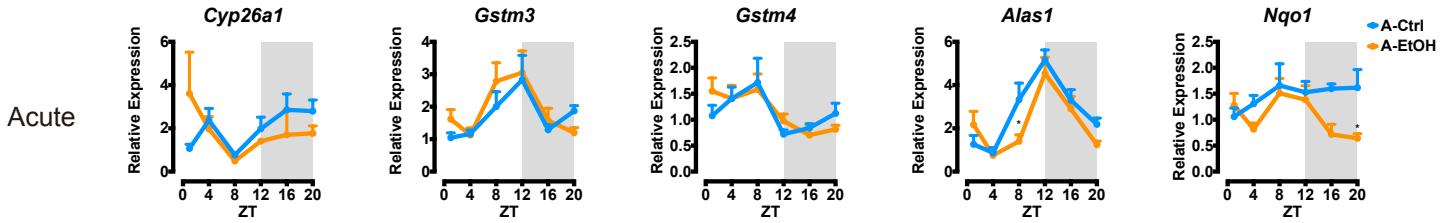
Acute
Cyp26a1
Gstm3
Gstm4
Alas1
Nqo1
Relative Expression
ZT
A-Ctrl
A-EtOH

C

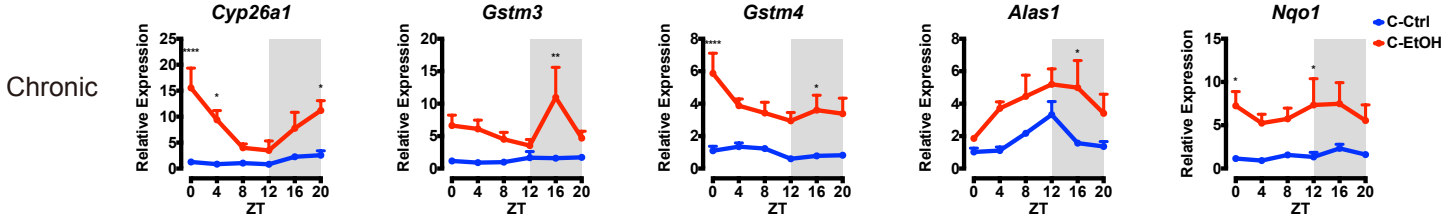
Chronic
Cyp26a1
Gstm3
Gstm4
Alas1
Nqo1
Relative Expression
ZT
C-Ctrl
C-EtOH

D

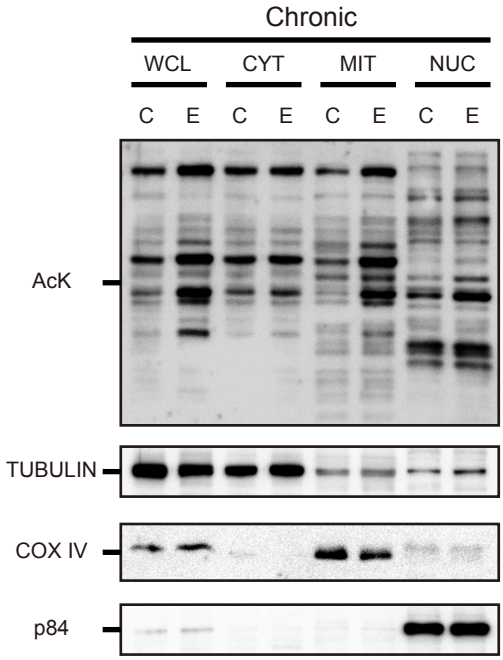
Chronic
WCL
CYT
MIT
NUC
C
E
C
E
C
E
C
E
AcK
TUBULIN
COX IV
p84

Fig. S5. Partitioning of metabolic enzymes acetylation and acetyl-CoA metabolism, related to Fig. 5.

(A) Gene Ontology analysis representing the top five biological processes enriched in up-regulated and down-regulated hepatic proteins (n = 4 per group) at ZT4 in chronic conditions from the proteomic analysis, with the number of proteins indicated on the graph (P value < 0.05). (B) Gene expression profiles of xenobiotic metabolism in acute ethanol (EtOH) feeding. (C) Gene expression profiles of xenobiotic metabolism in chronic ethanol (EtOH) feeding. Gene expression was normalized to 18S ribosomal RNA and presented as mean + SEM (n=4-6 biological replicates per time point per group). *P<0.05, **P<0.01, and ****P<0.0001 in ANOVA with Bonferroni post-hoc test. (D) Representative immunoblots of whole cell lysates (WCL), cytosolic (CYT), mitochondrial (MIT) and nuclear (NUC) fractions from chronic control (Ctrl) and ethanol (EtOH) livers. For loading and fraction quality, TUBULIN was used for the cytosol, COX IV for the mitochondria and P84 for the nucleus. AcK denotes acetylated lysine.

Dataset S1 (separate file). Row RPKM value of RNA-seq on acute alcohol experiment, Related to Figs. 2, 3, 4, S2.

Dataset S2 (separate file). Row RPKM value of RNA-seq on chronic alcohol experiment, Related to Figs. 2, 3, 4, S2.

Dataset S3 (separate file). Bio_CYCLE and Cyber-T analysis on acute alcohol experiment, Related to Figs. 2, 3, 4, S2.

Dataset S4 (separate file). Bio_CYCLE and Cyber-T analysis on chronic alcohol experiment, Related to Figs. 2, 3, 4, S2.

Dataset S5 (separate file). Acetylome analysis, Related to Fig. 5.

Dataset S6 (separate file). Proteome analysis, Related to Figs. 5, S5.

Dataset S7 (separate file). Primer sequence for Real-Time qPCR, Related to Figs. 4, S3, S5.

References

1. J. Gaucher *et al.*, Bromodomain-dependent stage-specific male genome programming by Brdt. *The EMBO journal* **31**, 3809-3820 (2012).
2. B. Cox, A. Emili, Tissue subcellular fractionation and protein extraction for use in mass-spectrometry-based proteomics. *Nature protocols* **1**, 1872-1878 (2006).
3. I. Dimauro, T. Pearson, D. Caporossi, M. J. Jackson, A simple protocol for the subcellular fractionation of skeletal muscle cells and tissue. *BMC research notes* **5**, 513 (2012).
4. D. Karolchik *et al.*, The UCSC Genome Browser Database. *Nucleic acids research* **31**, 51-54 (2003).
5. E. P. Consortium, The ENCODE (ENCyclopedia Of DNA Elements) Project. *Science (New York, N.Y.)* **306**, 636-640 (2004).
6. S. Masri *et al.*, Circadian acetylome reveals regulation of mitochondrial metabolic pathways. *Proceedings of the National Academy of Sciences of the United States of America* **110**, 3339-3344 (2013).
7. S. Peleg *et al.*, Life span extension by targeting a link between metabolism and histone acetylation in Drosophila. *EMBO reports* **17**, 455-469 (2016).
8. J. Cox *et al.*, Andromeda: a peptide search engine integrated into the MaxQuant environment. *Journal of proteome research* **10**, 1794-1805 (2011).

9. J. E. Elias, S. P. Gygi, Target-decoy search strategy for increased confidence in large-scale protein identifications by mass spectrometry. *Nature methods* **4**, 207-214 (2007).
10. F. Agostinelli, N. Ceglia, B. Shahbaba, P. Sassone-Corsi, P. Baldi, What time is it? Deep learning approaches for circadian rhythms. *Bioinformatics* **32**, 8-17 (2016).
11. M. E. Hughes, J. B. Hogenesch, K. Kornacker, JTK_CYCLE: an efficient nonparametric algorithm for detecting rhythmic components in genome-scale data sets. *Journal of biological rhythms* **25**, 372-380 (2010).
12. A. Subramanian *et al.*, Gene set enrichment analysis: a knowledge-based approach for interpreting genome-wide expression profiles. *Proceedings of the National Academy of Sciences of the United States of America* **102**, 15545-15550 (2005).
13. P. Baldi, A. D. Long, A Bayesian framework for the analysis of microarray expression data: regularized t -test and statistical inferences of gene changes. *Bioinformatics* **17**, 509-519 (2001).
14. M. A. Kayala, P. Baldi, Cyber-T web server: differential analysis of high-throughput data. *Nucleic acids research* **40**, W553-559 (2012).
15. W. Huang da, B. T. Sherman, R. A. Lempicki, Systematic and integrative analysis of large gene lists using DAVID bioinformatics resources. *Nature protocols* **4**, 44-57 (2009).
16. W. Huang da, B. T. Sherman, R. A. Lempicki, Bioinformatics enrichment tools: paths toward the comprehensive functional analysis of large gene lists. *Nucleic acids research* **37**, 1-13 (2009).
17. X. Xie, P. Rigor, P. Baldi, MotifMap: a human genome-wide map of candidate regulatory motif sites. *Bioinformatics* **25**, 167-174 (2009).
18. K. Daily, V. R. Patel, P. Rigor, X. Xie, P. Baldi, MotifMap: integrative genome-wide maps of regulatory motif sites for model species. *BMC bioinformatics* **12**, 495 (2011).
19. Y. Liu *et al.*, MotifMap-RNA: a genome-wide map of RBP binding sites. *Bioinformatics* **33**, 2029-2031 (2017).
20. V. R. Patel, K. Eckel-Mahan, P. Sassone-Corsi, P. Baldi, CircadiOmics: integrating circadian genomics, transcriptomics, proteomics and metabolomics. *Nature methods* **9**, 772-773 (2012).
21. V. R. Patel *et al.*, The pervasiveness and plasticity of circadian oscillations: the coupled circadian-oscillators framework. *Bioinformatics* **31**, 3181-3188 (2015).